molecular pharmaceutics

ACS AuthorChoice

Article

pubs.acs.org/molecularpharmaceutics

Terms of Use

# Toward a Rationale for the PTC124 (Ataluren) Promoted Readthrough of Premature Stop Codons: A Computational Approach and GFP-Reporter Cell-Based Assay

Laura Lentini,[†] Raffaella Melfi,[†] Aldo Di Leonardo,*[,†,‡] Angelo Spinello,[†] Giampaolo Barone,*[,†,§] Andrea Pace,*[,†,§] Antonio Palumbo Piccionello,[†] and Ivana Pibiri[†]

[†]Dipartimento di Scienze e Tecnologie Biologiche, Chimiche e Farmaceutiche, Università degli Studi di Palermo, Viale delle Scienze Ed. 17, 90128 Palermo, Italy

[‡]Centro di OncoBiologia Sperimentale (COBS), via San Lorenzo Colli, 90145 Palermo, Italy

[§]Istituto EuroMediterraneo di Scienza e Tecnologia (IEMEST), Via Emerico Amari 123, 90139 Palermo, Italy

Supporting Information

**ABSTRACT:** The presence in the mRNA of premature stop codons (PTCs) results in protein truncation responsible for several inherited (genetic) diseases. A well-known example of these diseases is cystic fibrosis (CF), where approximately 10% (worldwide) of patients have nonsense mutations in the CF transmembrane regulator (CFTR) gene. PTC124 (3-(5-(2-fluorophenyl)-1,2,4-oxadiazol-3-yl)-benzoic acid), also known as Ataluren, is a small molecule that has been suggested to allow PTC readthrough even though its target has yet to be identified. In the lack of a general consensus about its mechanism of action, we experimentally tested the ability of PTC124 to promote the readthrough of premature termination codons by using a new reporter. The reporter vector was based on a plasmid harboring the H2B histone coding sequence fused in frame with the green fluorescent protein (GFP) cDNA, and a TGA stop codon was introduced in the H2B-GFP gene by site-directed mutagenesis. Additionally, an unprecedented computational study on the putative supramolecular interaction between PTC124 and an 11-codon (33-nucleotides) sequence corresponding to a CFTR mRNA fragment containing a central UGA nonsense mutation showed a specific interaction between PTC124 and the UGA codon. Altogether, the H2B-GFP-opal based assay and the molecular dynamics (MD) simulation support the hypothesis that PTC124 is able to promote the specific readthrough of internal TGA premature stop codons.

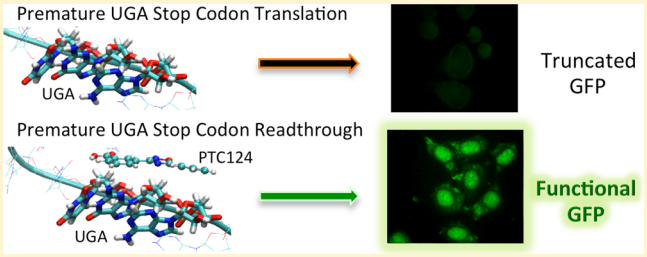


**KEYWORDS:** *cystic fibrosis (CF), Duchenne muscular distrophy (DMD), premature termination codons (PTC), nonsense mutation readthrough, oxadiazoles, ataluren, molecular dynamics (MD), green fluorescent protein (GFP)*

## INTRODUCTION

A nonsense mutation is a single nucleotide change in the DNA sequence that introduces a premature stop codon—UGA, UAG, or UAA, also named as opal, amber, and ochre, respectively—in the protein-coding region of the corresponding mRNA. Such premature termination codons (PTCs) cause inappropriate termination of translation producing truncated polypeptides and promote mRNA destabilization by nonsense-mediated mRNA decay (NMD). NMD is a surveillance pathway, triggered when ribosomes encounter a premature translation-termination codon, that rids the cell of mRNAs that are incompletely processed or that lack complete open reading frames, committing these transcripts to rapid degradation.[1,2] Nonsense mutations can cause anywhere from 5 to 70% of the individual cases of most inherited disease, including cystic fibrosis (CF), Duchenne muscular dystrophy (DMD), spinal muscular atrophy, hemophilia, neurofibromatosis, retinitis pigmentosa, lysosomal storage disease, Hurler's Syndrome, and a variety of other genetic disorders as well as of many forms of cancer.[3−6] In some cases, promoting the recovery of truncated protein by boosting functional protein synthesis to as little as 5% of normal levels may greatly reduce the severity or eliminate the principal manifestations of the disease.[7,8] Besides gene therapy, pharmacological approaches aiming at modifying gene expression by promoting the readthrough of nonsense mutations have gained interest in recent years.[9−11] For instance, aminoglycoside antibiotics can suppress stop codons by disturbing the normal proofreading function of the ribosome, leading to insertion of a near-cognate amino acid at a PTC thus translating a full-length protein.[12−14] Unfortunately, aminoglycoside action lacks specificity resulting in readthrough

**Received:** April 18, 2013
**Revised:** December 17, 2013
**Accepted:** January 31, 2014
**Published:** January 31, 2014

  

of many correctly positioned stop codons. Furthermore, a potential complication is the nephrotoxicity and ototoxicity of aminoglycoside during long-term treatments.[15]

Recently, a 1,2,4-oxadiazole derivatative (3-(5-(2-fluorophenyl)-(1,2,4-oxadiazol-3-yl)-benzoic acid), also known as PTC124 or Ataluren, was suggested to induce ribosomal readthrough of premature but not normal termination codons.[16] 1,2,4-Oxadiazoles[17] are a class of small molecules which have gained attention for their pharmaceutical properties[18−20] and potential application in materials.[21−24] Originally, PTC124 was selected on the basis of a high throughput screening based on firefly luciferase (Fluc) reporter assays.[16] The PTC124-induced readthrough was estimated in HEK293 cells transfected with a luciferase reporter gene (Luc190) harboring a PTC at Thr190, replacing the normal ACA with UAA, UAG, and UGA.[16] Additional assays supporting nonsense suppression were performed by evaluating the synthesis of full-length proteins, such as distrophin in mdx mice,[16,25−27] CFTR in transgenic mice,[25,26] and harmonin[9] in mice harboring a USH1C nonsense mutation.[28] Although mimicking the effect of aminoglycosides, PTC124 is not an antibiotic, exhibits lower toxicity, and has the advantage of specifically promoting the readthrough of nonsense mutations only, without affecting normally positioned termination codons.[16,25,29] PTC124 has a very strong safety profile;[30,31] however, despite initial promising results,[16,29] extended clinical studies on Duchenne/Becker muscular dystrophy (DMD/BMD) patients are currently underway to reach statistical significance.[31] On the other hand, PTC124 is still under clinical evaluation for the treatment of CF.[32,33] Indeed, patients affected by CF lack adequate levels of the cystic fibrosis transmembrane conductance regulator (CFTR) protein, and more than 1000 disease-causing mutations have been identified in CFTR. The most commonly observed mutations include deletion of a codon at position 508 (delta-F508), a missense mutation at position 551, and a nonsense mutation at position 542 (G542X).[34] Cystic fibrosis patients with nonsense-mutation essentially produce no CFTR protein, thus suffering a more severe form of the disease. Therefore, given the impact of PTCs within the CFTR gene, accounting for up to 10% of pathogenetic CF mutations in white populations and nearly 85% among individuals of Ashkenazi Jewish descent, the development of a nonsense readthrough strategy is highly demanded.[35] Quite surprisingly, in contrast with the increased number of studies on PTC124's ability to promote readthrough, the biomolecular target of PTC124 still needs to be fully established.[6,28,36] Besides the uncertainty regarding PTC124's target, doubts have been raised about the actual nonsense suppression mechanism, given the demonstrated interaction between PTC124 and the firefly luciferase used to test its readthrough efficacy.[37,38] Due to the demonstrated dual-activity of PTC124, which was selected through a FLuc based assay[16] but has shown also FLuc inhibition properties,[38] orthogonal assays (i.e., assays using a different reporter to confirm the same biological activity)[39] should be rigorously performed to verify its readthrough efficacy. In these cases, where the enzymatic nature of the FLuc reporter might be the cause of misinterpretable results, the use of nonenzymatic fluorescent reporters, such as the green fluorescent protein (GFP), has been recently suggested as ideal orthogonal test for reporter specific effects.[40]

In the attempt to shed light on the mechanism of action of PTC124 we decided to perform an orthogonal assay based on different reporters as recently suggested by Thorne et al.[39] Therefore, we developed a reporter plasmid (H2B-GFP-opal), based on the GFP harboring a PTC at Trp58, to be compared with the luciferase reporter gene (pFLuc190$^{UGA}$ by Auld et al.)[37] to confirm the nonsense suppression activity of PTC124.

While computational approaches have been developed to interpret the (16S) RNA-aminoglycoside interactions,[41] the lack of consensus about PTC124's mechanism of action has inhibited the development of any kind of *in silico* study. Therefore, we performed the first computational study to investigate putative codon-specific supramolecular interactions between the PTC124 and an 11 codon long sequence corresponding to the CFTR fragment coding mRNA bearing a G542X nonsense mutation (i.e., UGA at position 542).

## EXPERIMENTAL SECTION

**Chemistry.** IR spectra were registered with a Shimadzu FTIR-8300 instrument. $^1$H NMR spectra were recorded on a Bruker 300 Avance spectrometer, operating at 300 MHz, with TMS as an internal standard. Flash chromatography was performed by using silica gel (Merck, 0.040−0.063 mm) and mixtures of ethyl acetate and petroleum ether (fraction boiling in the range of 40−60 °C) in various ratios. All solvents and reagents were obtained from commercial sources. Compound **1**[42] and PTC124[16,37] had physical characteristics identical to those of the compounds prepared by alternative procedures as reported in the literature.

*3-Cyanomethylbenzoate (**1**).* 3-Cyanobenzoyl chloride (0.983 g, 5.93 mmol) was dissolved in MeOH (200 mL); then TEA was added (1.65 mL, 11.87 mmol) and the reaction was allowed to stir at room temperature for about 30 min. The solvent was removed under vacuum, and the reaction mixture was then diluted with water; the product, filtrated on Büchner, was obtained in 94% yield.

*Methyl-3-(N-hydroxycarbamimidoyl)-benzoate (**2**).* 3-Cyanomethylbenzoate (0.996 g, 6.16 mmol) was dissolved in MeOH (150 mL), hydroxylamine chlorohydrate (1.2 g, 17.2 mmol), and potassium *tert*-butoxide (1.9 g, 17.2 mmol) were added, and the reaction was allowed to stir at room temperature overnight. The solvent was removed under vacuum, and the residue was washed with water and filtrated on Büchner. Chromatography of the residue gave product **2** in 73% yield. IR (nujol): 3453, 3360, 3180, 1726 cm$^{-1}$; $^1$H NMR (300 MHz, DMSO-$d_6$): $\delta$ 9.85 (s, 1H), 8.36 (d, 1H; $J$ = 0.9 Hz), 8.01 (t, 1H; $J$ = 7.5 Hz), 7.59 (t, 1H; $J$ = 7.5 Hz), 6.03 (s, 2H), 3.93 (s, 3H).

*Methyl-3-(5-(2-fluorophenyl)-1,2,4-oxadiazol-3-yl)-benzoate (**3**).* Methyl-3-(*N*-hydroxycarbamimidoyl)-benzoate (0.250 g, 1.29 mmol) was dissolved in acetone (200 mL); $K_2CO_3$ (0.213 g, 1.54 mmol) and 2-fluorobenzoyl chloride (1.54 mmol) were added, and the reaction was allowed to stir at room temperature for 24 h.

The solvent was removed under vacuum; then the mixture was maintained under reflux in water for about 30 min in order to allow the cyclization of the precursor. The product, filtrated on Büchner, was obtained in 80% yield; IR (nujol): 1723 cm$^{-1}$; $^1$H NMR (300 MHz, DMSO-$d_6$): $\delta$ 8.78 (t, 1H, $J$ = 1.8 Hz), 8.31 (dt, 1H, $J_1$ = 7.8 Hz, $J_2$ = 1.4 Hz), 8.18−8.12 (m, 2H), 7.59−7.52 (m, 2H), 7.32−7.20 (m, 2H), 3.91 (s, 3H).

*3-(5-(2-Fluorophenyl)-1,2,4-oxadiazol-3-yl)-benzoic Acid (PTC124).* Methyl 3-(5-(2-fluorophenyl)-1,2,4-oxadiazol-3-yl)-benzoate **3** (0.34 mmol) was dissolved in benzene (40 mL); $BBr_3$ (4 mL, 13.7 mmol) was added, and the solution was

allowed to stir at 80 °C for 4h. After removal of the solvent under vacuum, the residue was treated with water and extracted with ethyl acetate. Chromatography of the residue gave PTC124 in 73% yield.

**Biology.** *Site Directed Mutagenesis and Clone Screening.* Mutagenesis of the H2B-GFP[43] vector to change the tryptophan codon (TGG) at position 172-4 of the GFP coding sequence to the TGA stop codon (opal) was performed with the QuickChange kit, Statagene, CA, USA. This approach required a high fidelity DNA polymerase which replicates both strand of the plasmid vector by extending two primers, both containing the desired mutation, each complementary to the same region but to opposite strands of the template. We used the high fidelity *Pfu-Turbo* DNA polymerase, 50 ng of plasmid template, and the following oligonucleotides:[44]

GFP opal fw 5′-GCTGCCCGTGCCCTGACCCACCCT-CGTGACC-3′

GFP opal rev 5′-GGTCACGAGGGTGGGTCAGGGC-ACGGGCAGC-3′

In each PCR cycle annealing and extension temperatures were, respectively, 58 °C for 1 min and 68 °C for 7 min. Following 12 cycles of amplification, the product was treated with *Dpn*I restriction enzyme. The *Dpn*I endonuclease (target sequence: 5′-Gm6ATC-3′) is specific for methylated and hemimethylated DNA and is used to digest the methylated parental DNA template (isolated from a dam+ *E. coli* strain) and to select for mutation-containing synthesized DNA. The resulting mutated plasmids were transformed into XL1-Blue supercompetent cells that were plated on LB agar plates with ampicillin. For the "Colony PCR" we used two primers internal to the H2B-GFP gene: GFP fw 5′-GTAAACGGCCAC-AAGTT-3′, and GFP 3′-rev 5′-CTTGTACAGCTCGTCC-ATG-3′. The PCR mix, containing the primers, the DNA polymerase, and the dNTPs, was added directly to the tubes containing a small amount of heat denatured bacteria picked from each colony and, after 30 cycles, 5 μL of PCR product were run on 1% agarose gel. DNA bands were revealed by ethidium bromide staining and UV exposition. Plasmid DNA was purified with NucleoSpin Plasmid miniprep kit (Macherey-Nagel) according to manufacturer instructions. For "selective PCR" we used forward primers with differing 3′ termini matching either the wild-type or the mutant nucleotide in order to allow selective amplification of the corresponding wild-type or mutant target DNA.[45] To the reaction we added a thermostable DNA polymerase lacking 3′ to 5′ proofreading activity (DyNAzyme II DNA Polymerase), purified plasmid DNA as template, and the primers GFP 3′G wt 5′-CTGCCCGTGCCCTGG-3′ and GFP 3′A opal 5′-GCTG-CCCGTGCCCTGA-3′. Reverse primer was the same in all samples (GFP 3′rev). Wild-type H2B-GFP gene was also amplified as a control. After 20 cycles (annealing temperature was 57 °C for 30 s), 5 μL of PCR product were run on 1% agarose gel and DNA bands visualized on a UV trans-illuminator. Pictures of the gels were taken with a digital camera (Canon). Plasmid DNA from positive clones was purified, and 1 μg was sent to Eurofins MWG Operon for sequencing.

*Cell Transfection and Measurement of Luciferase and GFP Activity.* HeLa cells were plated in a 12 multiwell plate, at a density of $1 \times 10^5$/mL in a volume of 1 mL per well, and transfected with wild type (pFLuc) and mutant (pFLuc190$^{UGA}$) plasmids by using lipofectamine 2000 (Invitrogen). Cells were then incubated for 24 h before the addition of 12 μM PTC124. After 24 h of treatment, the cells were washed with PBS and incubated with the detection mix Steady-Glo luciferase reagent (Promega). Aliquots of 200 μL of cell suspension were plated in triplicate in a 96 well. Luciferase activity was measured by a luminometer (Promega). Stably transfected (H2B-GFP wt and H2B-GFP-opal) HeLa cells were selected by antibiotic (blasticidin) resistance and characterized by PCR to verify the integrity of the reporter gene. Expression of the fusion protein in live cells after treatment with PTC124 (72 h) was monitored by fluorescence microscopy (ZEISS). All of the examined cells underwent identical treatment with the exception of drug concentration. Different brightness in microscopic images has to be attributed to the confluence of the cells.

*Genomic DNA Purification and Reporter Gene Control.* PureLink Genomic DNA Kit (Invitrogen) was used to isolate genomic DNA from the selected clones of HeLa H2B-GFP-opal. $3 \times 10^6$ cells were lysed, and the DNA was rapidly purified using a spin column based centrifugation procedure. To verify the integrity of the H2B-GFP reporter gene, 130 ng of genomic DNA were used as template for a PCR reaction. We used the EF1α forward primer: 5′-TCAAGCCTCAGACAGTGGTTC annealing to the gene promoter region, and the GFP 3′-rev primer annealing to the 3′ end of the gene. After 35 cycles of amplification 5 μL of PCR product was run on 1% agarose gel.

*Immunofluorescence Microscopy.* To visualize EGFP expression cells were grown on rounded glass coverslips and fixed with methanol 100% for 2 min, permeabilized with 0.01% TritonX (Sigma-Aldrich) in PBS for 15 min and blocked with 0.1% BSA for 30 min, both at room temperature. Coverslips were incubated overnight at 4 °C with a mouse monoclonal antibody against GFP (Sigma-Aldrich, diluted 5 μg/mL) derived from mice immunized with a synthetic peptide corresponding to amino acids 132−144 of the GFP from jellyfish *Aequorea victoria*, followed by a goat antimouse IgG-FITC secondary antibody (Sigma-Aldrich, diluted 1:200) for 1 h at 37 °C. Nuclei were visualized with 1 μg/mL of 4′,6-diamidino-2-phenylindole (DAPI) and examined on a Zeiss Axioskop microscope equipped for fluorescence, images were captured with a CCD digital camera (AxioCam, Zeiss) and then transferred to Adobe PhotoShop for printing.

**Cytofluorimetry.** Asynchronously growing cells were treated with PTC124 and G418 for 24 h. DNA content was determined using propidium iodide (PI) staining by treating cells with PBS solution containing 4 μg/mL of PI and 40 μg/mL RNase. Samples were analyzed on a FACSCanto (Becton Dickinson). Experiments were repeated at least twice; 10 000 events were analyzed by FACSDiva software (see Supporting Information).

*Western Blotting.* Protein concentration was measured using the Bio-Rad Protein Assay (Bio-Rad Laboratories) Proteins (50 μg) were separated by 10% SDS-PAGE containing 0.1% SDS and transferred to Hybond-C nitrocellulose membranes (Amersham Life Science) by electroblotting as described previously.[46] The membrane was incubated with anti-GFP mouse (Sigma-Aldrich, 2 μg/mL), as primary antibodies (Santa Cruz), and HRP-conjugated mouse rabbit IgG (Abcam, 1:5000), as secondary antibodies. The target protein was detected with enhanced chemiluminescence Western blotting detection reagents (PIERCE). Membrane was stained with Ponceau-Red to confirm equivalent loading of total protein in all lanes. We used also β-actin antibody (mouse; Sigma-Aldrich 1:10 000) to confirm proteins loading. Protein bands were

**Scheme 1. Synthesis of PTC124**

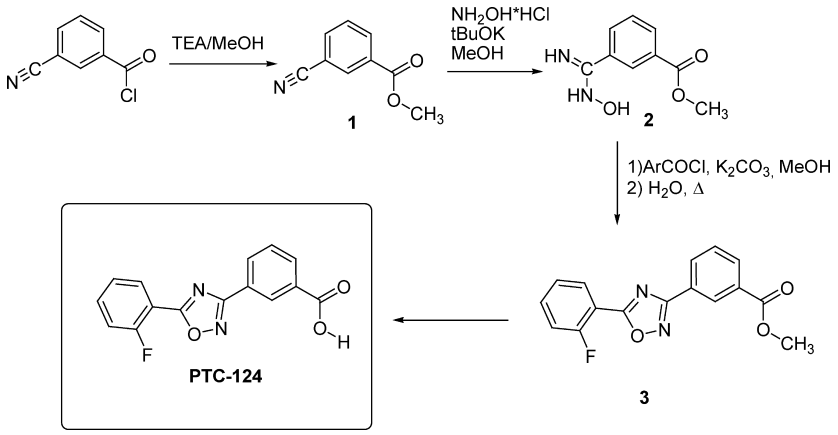


analyzed by ImageJ Software. Experiments were run in triplicate. Figure 5B shows a representative WB experiment. The Figure 5C graph reports the average value of the WB bands quantitation, and error bars were calculated as the standard deviation method.

**Computational Details.** The following four sequences of CFTR mRNA, each consisting of 33 ribonucleotides expressing aminoacids 537 through 547, either wild type or harboring a premature stop codon at position 542:

CFTR wt 5′-GACAAUAUAGUUCUUGGAGAAGGUGG-AAUCACA-3′,

CFTR-UGA 5′-GACAAUAUAGUUCUUUGAGAAG-GUGGAAUCACA-3′,

CFTR-UAG 5′-GACAAUAUAGUUCUUUAGGAAG-GUGGAAUCACA-3′,

CFTR-UAA 5′-GACAAUAUAGUUCUUUAAGAAG-GUGGAAUCACA-3′,

were constructed in the A conformation using the NUCLEIC routine of the TINKER program package[47] as recently described.[48,49] By considering the single nucleotides in the 33-nucleotides long fragment, the varying codon involves positions 16, 17, and 18. The topology file of the PTC124 molecule was generated using ACPYPE.[50−52] Molecular dynamics (MD) simulations were performed with the GROMACS 4.5.3 suite[53,54] using the AMBER ff99SB force field[55] with parmBsc0 nucleic acid torsions.[56]

Five MD simulations, each lasting 100 ns, were conducted to assess the supramolecular interactions between the four mRNA fragments described above and PTC124. The starting position of PTC124 ligand was varied by using the Maestro software.[57]

A triclinic box was added around the RNA and the ligand to a depth 1.5 nm on each side of the solute; this large value was necessary because of the large flexibility of the oligonucleotides. This box was filled with TIP3P water molecules, a solution density of about 1.03 g/mL was obtained. Thirty-two $Na^+$ counterions were added to neutralize the negative charges of the RNA backbone; other $Na^+$ and $Cl^-$ ions were added to achieve a solution ionic strength of about 0.15 M. Standard AMBER parameters were used for sodium ($\sigma$ = 0.33284 nm; $\varepsilon$ = 0.01159 kJ/mol) and chlorine ($\sigma$ = 0.44010 nm; $\varepsilon$ = 0.41840 kJ/mol). Simulations were performed in the canonical NVT ensemble, at the temperature of 300 K, using a velocity rescaling thermostat.[58] The particle mesh Ewald method (PME)[59] was used to describe the long-range electrostatics interactions. The time step was set to 2 fs, and all covalent bonds were constrained with the LINCS algorithm. Energy minimization was run for 5000 steps using the steepest descend algorithm. In a 500 ps equilibration the oligonucleotides were harmonically restrained with a force constant of 1000 kJ $mol^{-1}$ $nm^{-2}$ at 300 K, which was gradually lowered until no restrains were applied. Moreover, the formation of hydrogen bonds was analyzed using the g_hbond GROMACS tool.

## RESULTS

**Synthesis of PTC124.** Our synthetic approach toward PTC124 is different from previously reported methods[16] and was carried out, following the classical amidoxime route[17,60] for the synthesis of variously substituted 1,2,4-oxadiazole derivatives.[61−68]

The synthetic strategy involves the synthesis of the methyl ester of 3-cyanobenzoic acid **1** as the initial step. The reaction, performed in methanol at room temperature with triethylamine (TEA), allowed to obtain the methyl ester in very good yields (94%) (Scheme 1). Compound **1** was then reacted with hydroxylamine to obtain the methyl 3-(*N*-hydroxycarbamimidoyl)-benzoate **2** (73%). The cyclization into the oxadiazole ring has been performed in a one-pot procedure by reacting methyl 3-(*N*-hydroxycarbamimidoyl)-benzoate **2** in acetone with 2-fluorobenzoyl chloride in the presence of potassium carbonate. After 24 h at room temperature, the solvent was removed, and the residue refluxed in water, thus allowing final cyclization into oxadiazole derivative **3** (80%). Oxadiazole **3** was finally hydrolyzed in benzene with boron tribromide, producing PTC124 in good yield (73%) (Scheme 1).

**Construction of the Reporter Plasmid Harboring the Opal (TGA) Premature Termination Codon and Cell Transfection.** To assess the *in vitro* ability of PTC124 to promote nonsense mutation suppression, we isolated human cell lines stably expressing the H2B-GFP chimeric gene, either wild-type (control) or mutated by the presence of a TGA premature stop codon.[44] The used vector was the H2B-GFP plasmid harboring a reporter gene encoding for the codon-optimized enhanced GFP protein that localizes in the nucleosome thanks to its fusion to the human histone H2B.[43,69] To generate the H2B-GFP-opal plasmid, where a wild-type codon is transformed in a nonsense codon, a single nucleotide substitution was introduced in the GFP coding sequence by site-directed mutagenesis as described in the Experimental Section.[44] We confirmed plasmid presence in all of the obtained bacterial clones by "Colony PCR" (Figure 1A). A DNA fragment of the correct size was amplified from all


dx.doi.org/10.1021/mp400230s | *Mol. Pharmaceutics* 2014, 11, 653−664

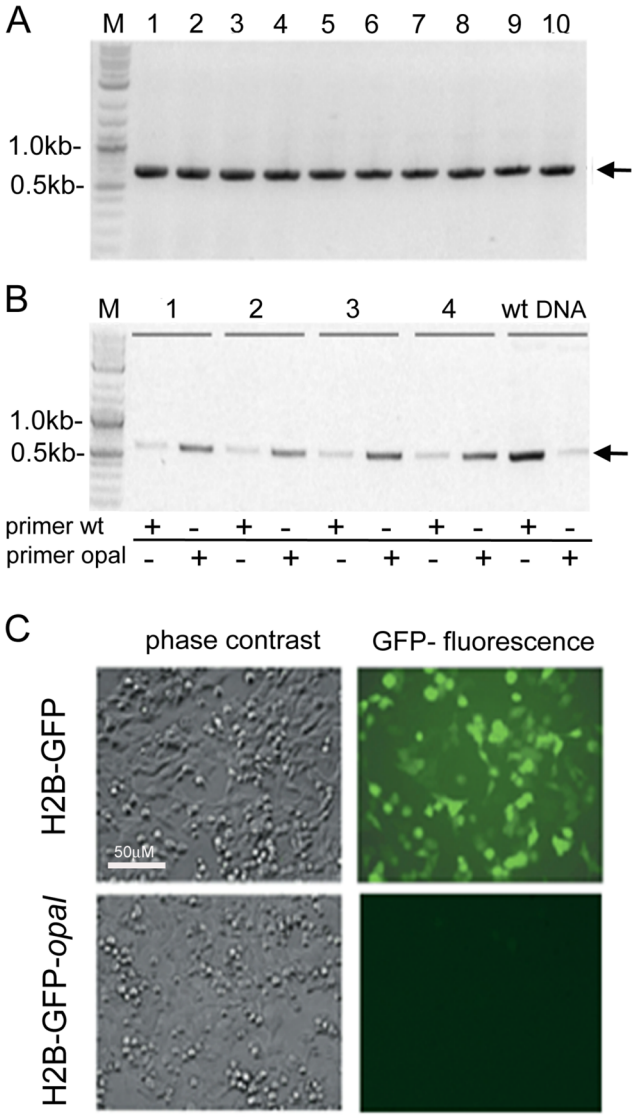


**Figure 1.** (A) "Colony PCR" with primers internal to the GFP gene on 10 bacterial clones (1−10). The arrow points the expected 650 bp amplicon. M: 2 log ladder. (B) "Selective PCR" with wt and opal mutant primers on purified plasmids from four randomly selected colonies (1−4) and on wt DNA (H2B-GFP plasmid). The arrow points the expected 560 bp amplicon. M: 2 log ladder. (C) Lack of fluorescence in H2B-GFP-opal transfected cell population.

samples (Figure 1B). Subsequently, HeLa cells were transfected with the H2B-GFP wild-type (control) and the H2B-GFP-opal (mutated) plasmids. HeLa cells transfected with the control vector showed high numbers of fluorescent cells, while those transfected with the mutated vector did not show any fluorescence (Figure 1C).

To minimize the possibility that lack of fluorescence in H2B-GFP-opal transfected cells might be due to plasmid rearrangement during the integration into the cellular DNA, transfected cells were cultured in presence of blasticidin, to select cells stably expressing H2B-GFP-opal. Following two weeks of selection, 20 cell clones were isolated and analyzed by polymerase chain reaction (PCR). Integrity of the reporter gene in the genomic DNA from these randomly selected clones was verified by PCR with primers annealing to the gene promoter and to the 3′ end of the gene (Figure 2). We also amplified the H2B-GFP gene from the wild type plasmid (C+)

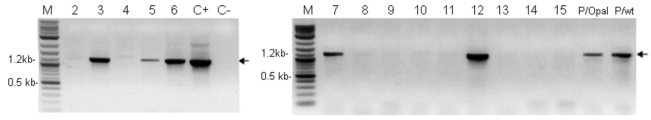


**Figure 2.** PCR analysis on genomic DNA extracted from randomly selected cell clones (2−6 and 7−15) with primers immediately adjacent to the H2B-GFP chimeric gene. Arrows point the expected amplicon of 1.2 kb. M: 2 log ladder. C+: H2B-GFP plasmid. C-: PCR mix. P/opal: H2B-GFP-opal cell population. P/wt: H2B-GFP wild type cell population.

and wild type and opal cell population (P/wt and P/opal) as positive controls. Negative control (C−) was the amplification mix. As expected, this analysis revealed that both populations presented cell clones with a 1.2 kb whole H2B-GFP gene, but only clones # 3, 5, 6, 7, and 12 were positive among those tested (Figure 2).

**PTC124 Treatments of Transfected Cells.** To ascertain that the synthesized PTC124 molecule was able to promote the readthrough of PTCs we used the FLuc cell-based assay[16] as a control. To this aim we transfected HeLa cells transiently with two specific plasmids: pFLuc-WT and pFLuc190$^{UGA}$ (courtesy of Professor J. Inglese)[37] and measured FLuc gene expression by luminescence. HeLa cells transfected with the pFLuc-WT plasmid showed high levels of luciferase activity (data not shown) confirming the correct functioning of the assay. After 24 h from transfection the pFLuc190$^{UGA}$ transfected cells were treated for additional 24 h with 12 $\mu$M PTC124. Following PTC124 exposition pFLuc190$^{UGA}$ transfected HeLa cells showed an increase of luciferase activity (Figure 3), this result is consistent with what previously published.[16]

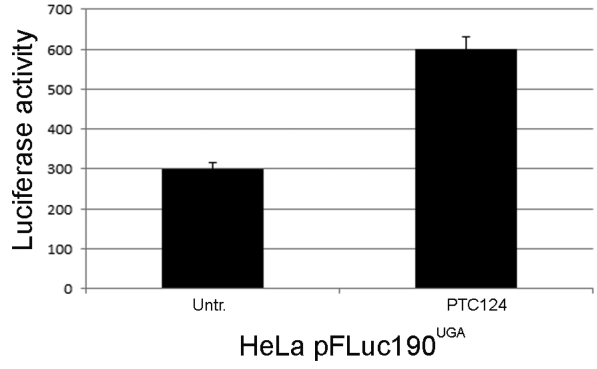


**Figure 3.** Histogram showing luciferase activity in HeLa FLuc-opal cells after exposition to PTC124 for 24 h.

To evaluate if PTC124 was able to promote the readthrough of premature stop codons also in HeLa cells stably transfected with the H2B-GFP-opal reporter vector, we performed a cytofluorimetric assay using known G418 as a reference readthrough promoting drug (see also Supporting Information). However, while wild type H2B-GFP was clearly detectable even with a small amount (5%) of fully fluorescent cells, fluorescence was not detectable in the case of H2B-GFP-opal treated with either G418 or PTC124, likely due to a small amount of protein resulting from the readthrough in each cell. Nevertheless, we were able to monitor the expression of the H2B-GFP fusion protein on a cell base by fluorescence microscopy on live cells. In fact, the presence of green fluorescence in cells would confirm the occurrence of a readthrough leading to a functional GFP. After exposition of

HeLa cells to 6 μM, 9 μM, and 12 μM PTC124 we observed the presence of green cells (Figure 4) indicating that PTC124

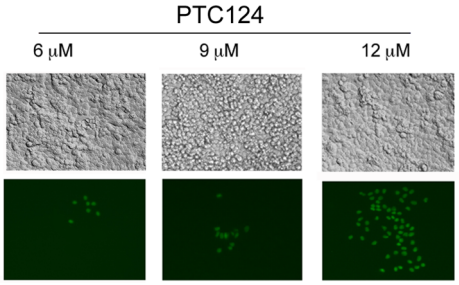


**Figure 4.** Expression levels of the H2B-GFP protein in H2B-GFP-opal transfected HeLa cells after 72 h of exposition to 6, 9, and 12 μM PTC124.

induced the production of a full length functional H2B-GFP protein, despite the presence of a premature stop codon in its coding sequence, as evidenced by the clearly dose-dependent increase in the number of green cells.

Live cells experiment suggested the dose dependency of the readthrough. However the amount of readthrough was not sufficient to reach full response from GFP fluorescence and obtain quantitative data. Therefore, to confirm this result we extended the investigation to the study of the recoding effects of PTC124 treatment by Western blotting and immunofluorescence analyses detecting H2B-GFP expression levels in HeLa cells stably transfected with the H2B-GFP-opal construct. As a positive control, H2B-GFP-opal cells were treated for 24 h with several concentrations of the aminoglycoside G418 (Figure 5A) that was previously shown to be able to recode stop codons.[70] Immunofluorescence microscopy done in H2B-GFP-opal transfected HeLa cells revealed the presence of positive cells for the H2B-GFP protein induced by G418 as well as by PTC124 (Figure 5A). The presence of green signals (GFP) in the cytoplasm of the cells treated with either G418 or PTC124 is indicative that translation of a "recoded" mRNA occurred. Because of the inherently difficulty of nonsense suppression, it is possible that the readthrough by a near cognate tRNA will result in a full-length protein not necessarily possessing the complete features of the wild-type fusion protein. To evaluate the suppression of the UGA stop codon and the presence of a full length H2B-GFP fusion protein, the cells were incubated with a mouse monoclonal antibody targeting aa132−144 of GFP. These aminoacids are downstream of the UGA premature termination codon replacing the codon for the amino acid tryptophan at position 58 of GFP protein. These immunofluorescence experiments confirmed that the readthrough of the PTC leads to a functional protein since green fluorescence is mainly observed into the nucleus. Next, the amount of H2B-GFP protein resulting from PTC124 treatment was measured by Western blot analysis (Figure 5B,C). The H2B-GFP-opal population was treated with 300 μg/mL of G418 and with 12 μM PTC124 for 24 h. Western blotting experiments indicated that the treatment with PTC124 induced the recovery of H2B-GFP protein (3- to 5-fold increase) in H2B-GFP-opal transfected HeLa cells. This increase was comparable to that obtained in cells treated with G418.

**Molecular Dynamics Simulations.** Since PTC124 affects the translational machinery, with a specific preference toward premature stop codons, we hypothesized mRNA as its plausible target. Unfortunately, the scarce water solubility of PTC124 rendered impracticable any experimental approach to verify such interaction by standard spectroscopic methods. Therefore, the possible interactions between PTC124 and mRNA were simulated by MD. Five MD simulations of 100 ns were conducted on the complex between the 1,2,4-oxadiazole ligand (PTC124), and four models of mRNA constituted by a sequence of 33 ribonucleotides of the CFTR gene, that differ in the identity of the central codon normally expressing aminoacid 542: (i) GGA, as found in the wild type mRNA; (ii) UGA, mimicking the G542X nonsense mutation; (iii) UAG, and (iv) UAA, representing the other two types of premature stop codons.

Considering the higher efficacy of PTC124 in promoting the readthrough of the premature UGA codon,[16] two MD simulations with PTC124 and CFTR-UGA were performed by positioning the ligand either "near" the center of the mRNA fragment (i.e., closer to the UGA codon) or "far" from the stop codon (i.e., near the 5′ end of the mRNA fragment). On the other hand, MD simulations involving PTC124 and either CFTR wt fragment, CFTR-UAG, or CFTR-UAA, started with the ligand already positioned near the center of the box and close to the 16-17-18 nucleotides in the mRNA fragment (see Computational Details).

The minimum distance between the PTC124 ligand and the 16−17−18 nucleotides (central codon) of the four mRNA fragments is plotted as a function of time in Figure 6. UGA1 and UGA2 refer to the two different MD simulations involving the CFTR-UGA mRNA fragment and PTC124 starting from the "near" and "far" initial position, respectively. Snapshots of the equilibrium arrangements are shown for all simulations in Figures 7−11.

These data clearly show that the two simulations involving the U16-G17-A18 codon lead to the shortest interaction distance at the equilibrium. The latter was reached much earlier (at about 20 ns) for the trajectory starting near the codon (UGA1, black line in Figure 6) and later (at about 70 ns) for the trajectory starting at the 5′ terminus of the mRNA fragment (UGA2, red line in Figure 6). Surprisingly, despite the different final arrangement (see Figures 7 and 8 below), the minimum distance reached at the equilibrium was essentially the same of about 2 Å. Similarly to UGA1 simulation, in the simulated interaction with the wild type mRNA fragment (GGA, blue line in Figure 6), PTC124 was initially placed near the GGA central codon. However, in this case, after initial fluctuations with distances up to 50 Å from the central codon, the ligand never approached the central codon and reached its equilibrium at about 90 ns with a minimum distance of about 6.5 Å. Remarkably, simulations involving the other two types of stop codons (UAG and UAA, green and magenta lines, respectively, in Figure 6) resulted in a higher equilibrium distance, even though PTC124 approached the central stop codon sporadically at about 5 ns (for both UAG and UAA) and 15 and 60 ns (for UAG). These findings seems to agree with the reported lower readthrough activity of PTC124 toward UAG and UAA premature stop codons.[16,28]

In our computational study of the interaction between PTC124 and the RNA model we have performed several MD simulations and focused our attention on the structures that more frequently occurred along the simulation. The driving forces toward the final equilibrium arrangement are based on stacking, H-bonding, and hydrophobic van der Waals interactions involving PTC124 and the nucleotides in the mRNA fragment. Simulation snapshots showing each type of

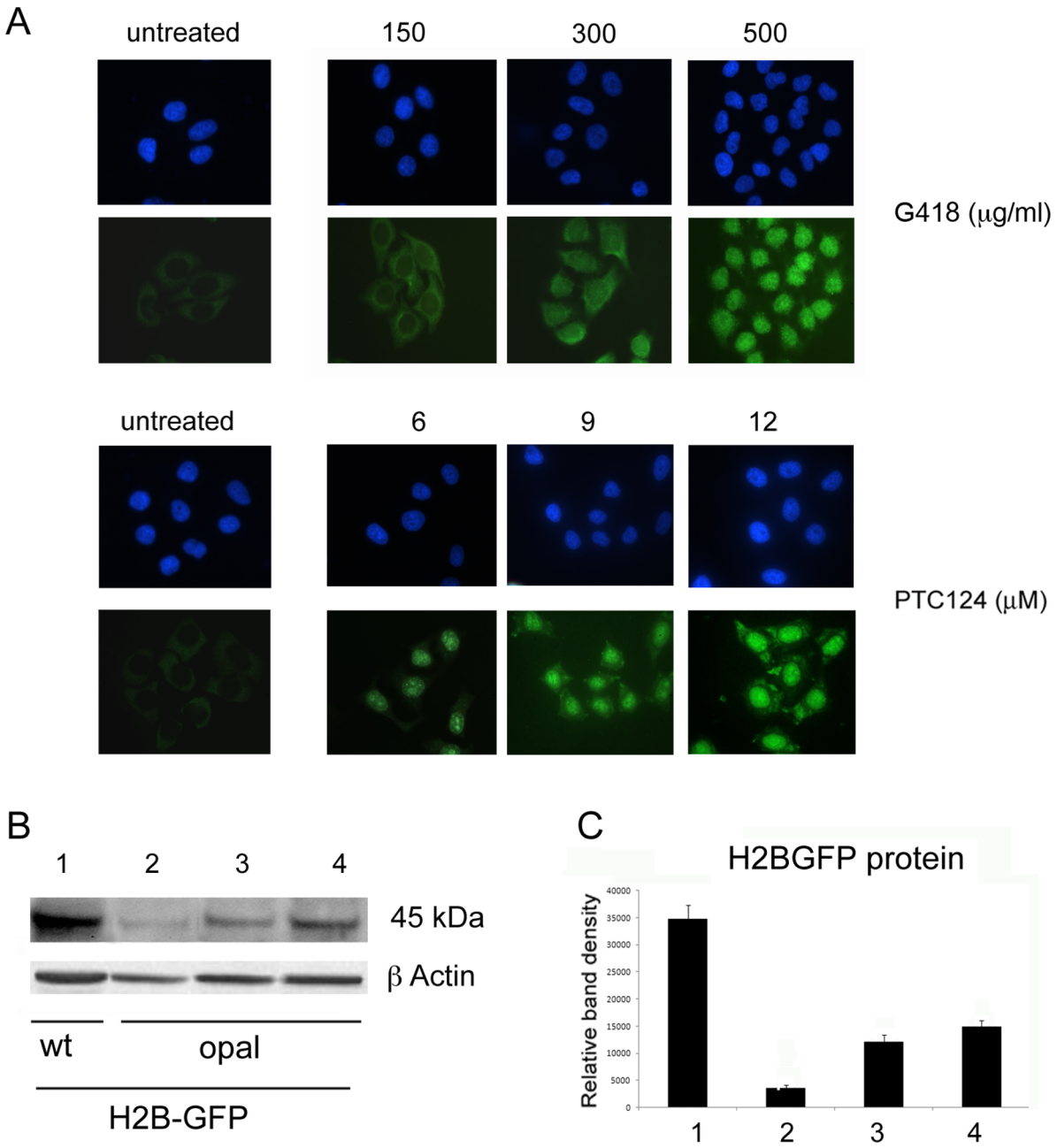


**Figure 5.** (A) Immunofluorescence analysis of the H2B-GFP protein in H2B-GFP-opal transfected HeLa cells after 24 h exposition to G418 and PTC124. (B) Western blot analysis showing H2B-GFP protein levels in HeLa cells expressing H2B-GFP wt (lane 1), and HeLa cells expressing H2B-GFP-opal left untreated (lane 2) or treated for 24 h with either G418 (lane 3) or PTC124 (lane 4). $\beta$-actin was used as a loading control. (C) Densitometry analysis of the Western blot bands in B shows H2B-GFP relative protein levels in transfected HeLa cells: (1) H2B-GFP wt; (2) H2B-GFP-opal (untreated); (3) H2B-GFP-opal treated with G418 (24 h); (4) H2B-GFP-opal treated with PTC124 (24 h).

these stabilizing interactions are illustrated in Figures 7 and 8. In particular, the equilibrium arrangement of the PTC124/mRNA complex from UGA1 simulation shows a stable van der Waals interaction between the PTC124 and the UGA codon, further stabilized by stacking $\pi-\pi$ interactions involving the aryl moieties of PTC124 with either G10 (Figure 7a) or both U12 and G10 (Figure 7b).

H-bond interactions are more evident in the case of UGA2 simulation (starting far from the central codon) leading to a final arrangement where the carboxylic moiety of PTC124 strongly interacts with the adenine A18 (Figure 8a). The number of H-bonds with a particular sequence, in particular with the UGA sequence, has been chosen to visualize the more frequently occurring interactions in the series of MD snapshots. A comparison between the total number of H-bond interactions, involving PTC124 with any part of the mRNA fragment during the entire 100 ns time frame (Figure 8b), with the number of H-bond interactions specifically involving the central UGA codon (Figure 8c) clearly supports the specificity of the interaction between PTC124 and UGA. For the first 70–75 ns, PTC124 occasionally interacts with the RNA fragment through one H-bond (rarely two) without involving the UGA codon. Interestingly, when PTC124 approaches the UGA codon after approximately 70–75 ns (see Figure 6, red line), interactions specifically involving the UGA codon become stably present through one, and occasionally two, H-bonds.


dx.doi.org/10.1021/mp400230s | *Mol. Pharmaceutics* 2014, 11, 653–664

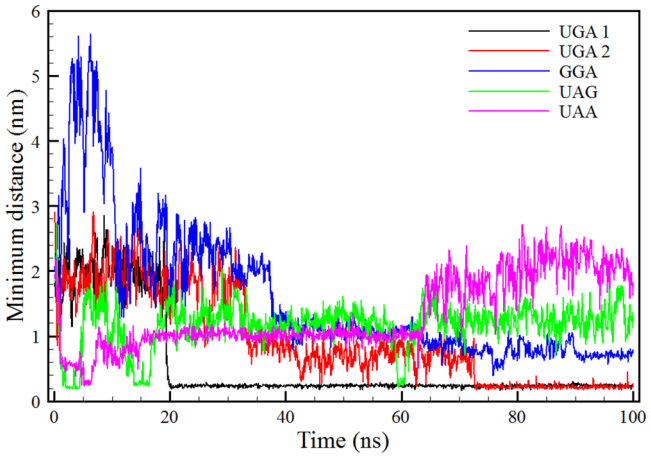


**Figure 6.** Variation of the minimum distance between PTC124 and the central (16-17-18) codon of the mRNA fragment during each 100 ns MD simulation.

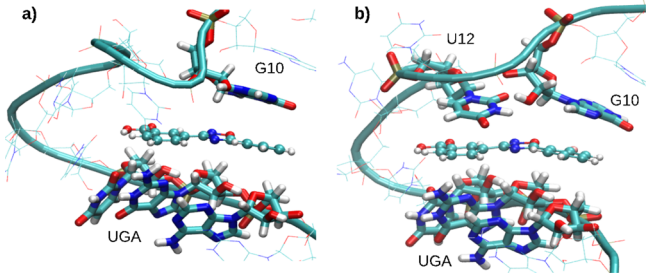


**Figure 7.** Two different snapshots at the equilibrium of the same UGA1MD simulation of interactions between PTC124 and a 33 nucleotide long CFTR-UGA mRNA fragment (water molecules not shown). Nucleotide numbering refers to the fragment (see computational details in the Experimental Section).

In the absence of an UGA codon, stacking interactions seem to prevail in driving the formation of the PTC124/mRNA complex. Interestingly, adenine was never involved in these stacking interactions. Particularly stable sandwich-like substructures were formed with PTC124 intercalated between a guanine and a uracil (Figures 9 and 10b) or two guanines (Figure 10a). However, due to the flexibility of the terminal endings of the 33 nucleotide long mRNA fragment, some caveat must be considered when interpreting the stacking interactions involving guanine at the terminal G1 or G33 position. These are found in simulations involving the wild type CFTR (Figure 9) and the CFTR-UAG (Figure 10a).

Finally, an MD simulation involving the CFTR-UAA mRNA fragment did not reach an equilibrium within the allotted 100 ns time frame. Indeed, after maintaining for more than 40 ns a position at about 10 Å distance from the UAA triplet (Figure 11a), PTC124 moves even farther from the central codon (Figure 11b) than observed in the other simulations.

## DISCUSSION

PTC124 (Ataluren) is a small molecule that has been suggested to allow PTC readthrough in the mRNA of different genetic disorders and in a manner similar to that of gentamicin but without the toxicity of an aminoglycoside.[16,25] However, it was also reported that PTC124's activity observed by *in vitro* experiments could be attributed to posttranslational stabilization of the luciferase itself, used as a reporter, and not to a true

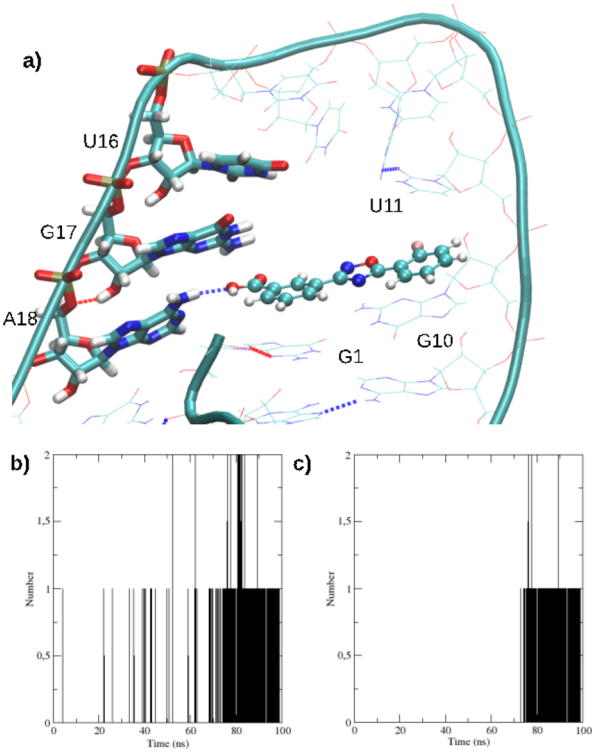


**Figure 8.** (a) Snapshot at the equilibrium of the UGA2MD simulation of interactions between PTC124 and a 33 nucleotide long CFTR-UGA mRNA fragment (water molecules not shown). Nucleotide numbering refers to the fragment (see computational details in the Experimental Section). (b) Number of H-bond interactions between PTC124 and any portion of the mRNA fragment during the 100 ns simulation. (c) Number of H-bond interactions between PTC124 and UGA in the mRNA fragment during the 100 ns simulation.

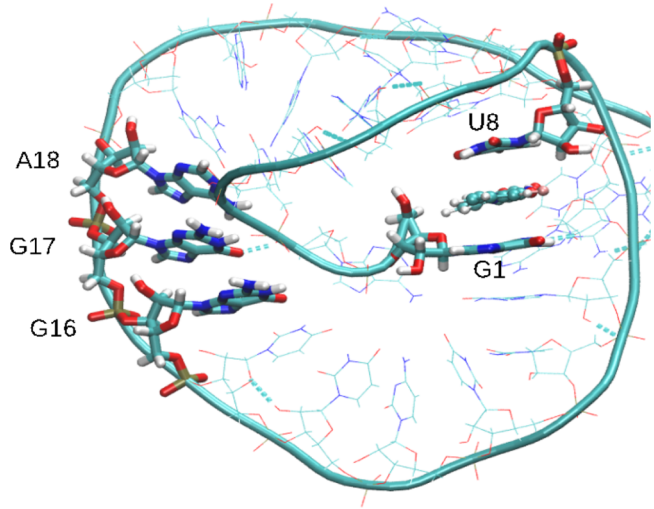


**Figure 9.** Snapshot at the equilibrium of GGA MD simulation of interactions between PTC124 and a 33-nucleotides long CFTR wild type mRNA fragment. Nucleotide numbering refers to the fragment (see computational details in the Experimental Section).

readthrough mechanism.[37] Indeed our orthogonal cell based assays, aimed to understand PTC124's mechanism of action by using a different reporter than the FLuc190$^{UGA}$ plasmid previously used,[16,25] indicated that PTC124 was able to induce, in a dose-dependent manner, a significant recovery of GFP's


dx.doi.org/10.1021/mp400230s | *Mol. Pharmaceutics* 2014, 11, 653−664

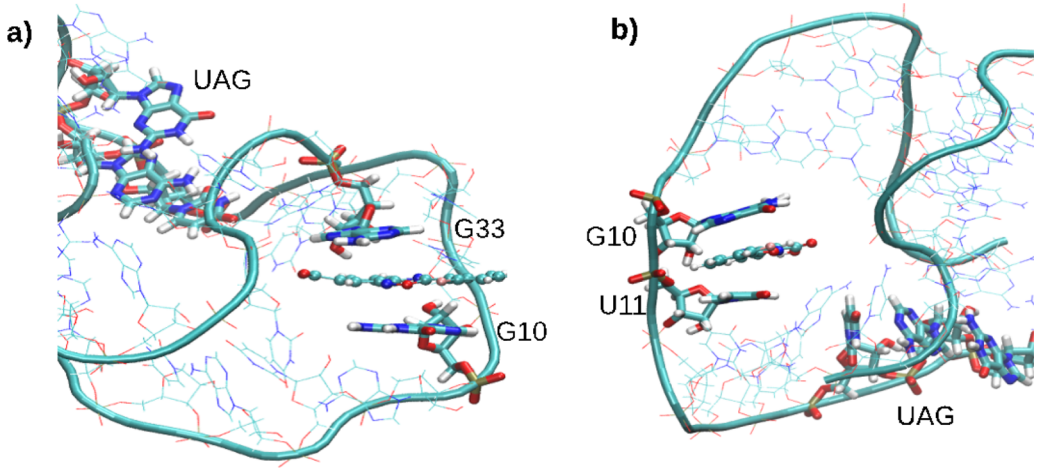


**Figure 10.** Two different snapshots at the equilibrium of the UAG MD simulation of interactions between PTC124 and a 33 nucleotide long CFTR-UAG mRNA fragment (water molecules not shown). Nucleotide numbering refers to the fragment (see computational details in the Experimental Section).

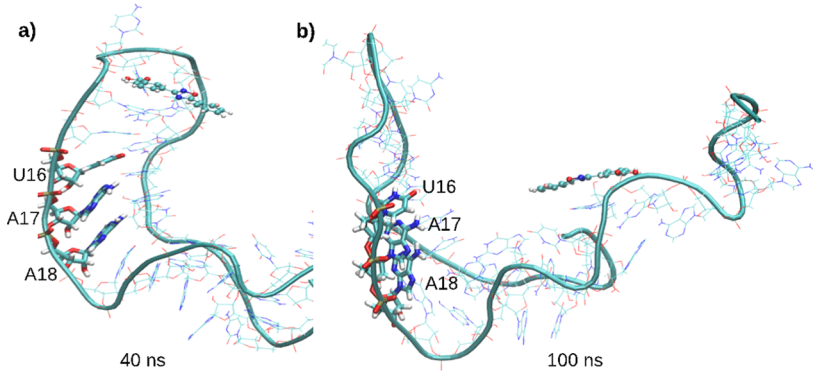


**Figure 11.** Two different snapshots of the UAA MD simulation showing no interaction between PTC124 and a 33 nucleotide long CFTR-UAA mRNA fragment (water molecules not shown). Nucleotide numbering refers to the fragment (see computational details in the Experimental Section). (a) Snapshot at 40 ns. (b) Snapshot at 100 ns.

fluorescence in cells transfected with the mutated reporter (H2B-GFP-opal). In addition, Western blotting experiments showed that the amount of H2B-GFP protein was similar following G418 and PTC124 treatment in cells transfected with the mutated reporter. This last finding reinforces the hypothesis that readthrough and not stabilization of the protein encoded by the reporter (H2B-GFP-opal) is the mechanism responsible for the recoding of the internal TGA premature stop codon.

The computational identification of the unknown biological target of a given compound is one of the "Sorcerer's Stone" of the pharmaceutical designer aiming at understanding the mechanism of action of a drug. In our MD simulations, which were based on the experimental evidence that PTC124 is able to affect the ribosomal translational machinery, we aimed at verifying if putative supramolecular interactions between mRNA and PTC124 could be the cause of the selective action of PTC124 to promote the readthrough particularly of UGA premature termination codons. Indeed, MD results showed that stable mRNA-PTC124 complexes can be formed specifically through the interaction with the UGA sequence (Figure 6). On the other hand, MD simulations clearly show that the proximity of PTC124 to the UAG and UAA premature stop codon occurs occasionally and at a longer distance with respect to the closer and more stable UGA interactions. In our opinion, the molecular recognition by PTC124 of a premature UGA should be aided by the presence of neighboring nucleobases.

In one complex (Figure 7) PTC124 completely masks the UGA codon through stable van der Waals and $\pi-\pi$ stacking interactions. If this interaction happens also in the ribosome, it might hinder the UGA recognition by the release factor.[71] In fact, the dimensions of PTC124, in its stable flat conformation, almost match the entire U16-G17-A18 distance (Figure 7) justifying also why PTC124 is not able to promote the readthrough of multiple sequential stop codons.[28]

The recognition of the UGA codon by the corresponding release factor would be encumbered also in the case of the other complex observed *in silico* between PTC124 and the CFTR-UGA mRNA fragment, where H-bonding involves the adenin of the stop codon (Figure 8). Additionally, given the very short distance (2 Å) between PTC124 and UGA, and the quasi-planar masking position that PTC124 assumes in one of these complexes (Figure 7), it is not excluded that a near-cognate tRNA, whose anticodon region is able to "recognize" PTC124, can still approach the ribosome in correspondence of the UGA triplet and perform its recoding leading to a functional full length protein.

At this stage, we cannot exclude that PTC124 would be able to interact also with an out-of-frame UGA in free mRNA aqueous solution. However, during the translation, any out-of-


dx.doi.org/10.1021/mp400230s | *Mol. Pharmaceutics* 2014, 11, 653−664

frame UGA in a mRNA molecule would be only partially positioned on the A site, thus making the binding with PTC124 ineffective and allowing a correct translation of the mRNA. Additionally, we cannot exclude that, similarly to aminoglycosides,[28] PTC124 is able to interact *in vivo* with specific nucleotides of the 18SrRNA in the ribosome, thus allowing the readthrough of the premature termination codon by a near-cognate tRNA.

## CONCLUSIONS

PTC124 (Ataluren) is one of the lead compounds in pharmacological approaches proposed to directly overcome nonsense mutations that are responsible of several genetic diseases such as cystic fibrosis and Duchenne muscular distrophy. Our work focused on PTC124 as a functional model for the interaction with a ribonucleotide sequence corresponding to a mRNA fragments of the CFTR gene, containing the UGA nonsense mutation, present in a subset of CF patient with the main objective to understand its mechanism of action. PTC124's readthrough activity was evaluated by using orthogonal assays with two different reporters: H2B-GFP-opal, based on the green fluorescent protein harboring a PTC at Trp58, and the luciferase reporter gene Luc190. Results support the hypothesis that PTC124 is able to promote the readthrough of the internal TGA premature stop codon, rather than simply stabilize proteins structures. Although the individuation of the actual PTC124's biological target is still a challenging goal, the possibility to simulate drug-target interactions at the molecular level in conjunction with experimental biology assays is a very promising synergic approach toward the definition of PTC124's mechanism of action. Additionally, a computational approach has been used for the first time to study mRNA as a putative target for PTC124 and to propose a reasonable interpretation of PTC124's specificity/selectivity toward a given UGA codon. Even if MD results represent a simplified model of the mRNA/PTC124 interactions in aqueous media, our data would be a useful starting point for computational studies of PTC124's behavior in much more complex systems such as the actual mRNP in the midst of a ribosome. Indeed, in a very recent paper debating the lack of PTC124 efficacy with a given set of reporter assays, mRNA regulatory processes has been mentioned as potentially involved in the mechanism through which PTC124 exerts its readthrough activity.[72] Prospectively, the interpretation at the molecular level of the interactions between PTC124 and its biological target will allow the design and synthesis of new molecules, structurally related to PTC124 and based on its mechanism of action, to promote a better readthrough of the other two premature stop codons, UAG and UAA, for which PTC124 showed a lower activity.

## ASSOCIATED CONTENT

### Supporting Information

Description of cytofluorimetric experiments. This material is available free of charge via the Internet at http://pubs.acs.org.

## AUTHOR INFORMATION

### Corresponding Authors

*A.P.: contact about chemical aspects and supramolecular interactions. Tel.: +39 091 23897543. Fax: +39 091 596825. E-mail: andrea.pace@unipa.it.

*A.D.L.: contact about biological aspects. Tel.: +39 091 23897340. Fax: +39 091 6577210. E-mail: aldo.dileonardo@unipa.it.

*G.B.: contact about computational aspects. Tel.: +39 091 23897973. Fax: +39 091 596825. E-mail: giampaolo.barone@unipa.it.

### Notes

The authors declare no competing financial interest.

## ACKNOWLEDGMENTS

This work was funded by the Italian Cystic Fibrosis Research Foundation, grant FFC no. 2/2011, with the contribution of Delegazione di Lecce, Delegazione di Vittoria (Ragusa) to Aldo Di Leonardo. We thank Prof. J. Inglese, NIH Chemical Genomics Center, National Institutes of Health, Bethesda, for kindly providing us with the FLuc190$^{UGA}$ plasmid. We gratefully acknowledge the CINECA award no. IsB05, year 2012, under the ISCRA initiative, for the availability of high performance computing resources and support.

## REFERENCES

(1) Baker, K. E.; Parker, R. Nonsense-mediated mRNA decay: terminating erroneous gene expression. *Curr. Opin. Cell Biol.* **2004**, *16*, 293−399.

(2) Maquat, L. E. Nonsense-mediated mRNA decay in mammals. *J. Cell. Sci.* **2005**, *118*, 1773−1776.

(3) Mendell, J. T.; Diez, H. C. When the Message Goes Awry: Disease-Producing Mutations that Influence mRNA Content and Performance. *Cell* **2001**, *107*, 411−414.

(4) Bordeira-Carriço, R.; Pego, A. P.; Santos, M.; Oliveira, C. Cancer syndromes and therapy by stop-codon readthrough. 2012, *18*, 667-678.

(5) Moosajee, M.; Gregory-Evans, K.; Ellis, C. D.; Seabra, M. C.; Gregory-Evans, C. Y. Translational bypass of nonsense mutations in zebrafish rep1, pax2.1 and lamb1 highlights a viable therapeutic option for untreatable genetic eye disease. *Hum. Mol. Genet.* **2008**, *17*, 3987−4000.

(6) Bidou, L.; Allamand, V.; Rousset, J.-P.; Namy, O. Sense from nonsense: therapies for premature stop codon diseases. *Trends Mol. Med.* **2012**, *18*, 679−688.

(7) Kerem, E. Pharmacologic therapy for stop mutations: how much CFTR activity is enough? *Curr. Opin. Pulm. Med.* **2004**, *10*, 547−552.

(8) Ramalho, A. S.; Beck, S.; Meyer, M.; Penque, D.; Cutting, G. R.; Amaral, M. D. Five Percent of Normal Cystic Fibrosis Transmembrane Conductance Regulator mRNA Ameliorates the Severity of Pulmonary Disease in Cystic Fibrosis. *Am. J. Respir. Cell Mol. Biol.* **2002**, *27*, 619−627.

(9) Goldmann, T.; Overlack, N.; Moeller, F.; Belakhov, V.; van Wyk, M.; Baasov, T.; Wolfrum, U.; Nagel-Wolfrum, K. A comparative evaluation of NB30, NB54 and PTC124 in translational readthrough efficacy for treatment of an USH1C nonsense mutation. *EMBO Mol. Med.* **2012**, *4*, 1186−1199.

(10) Extance, A. Targeting RNA: an emerging hope for treating muscular dystrophy. *Nat. Rev. Drug Discovery* **2009**, *8*, 917−918.

(11) Rowe, S. M.; Clancy, J. P. Pharmaceuticals Targeting Nonsense Mutations in Genetic Diseases. *Biodrugs* **2009**, *23*, 165−174.

(12) Hermann, T. Aminoglycoside antibiotics: old drugs and new therapeutic approaches. *Cell. Mol. Life. Sci.* **2007**, *64*, 1841−1852.

(13) Mc Coy, L. S.; Xie, Y.; Tor, Y. Antibiotics that target protein synthesis. *WIREs RNA* **2011**, *2*, 209−232.

(14) Malik, V.; Rodino-Klapac, L. R.; Viollet, L.; Mendell, J. R. Aminoglycoside-induced mutation suppression (stop codon read-through) as a therapeutic strategy for Duchenne muscular dystrophy. *Ther. Adv. Neurol. Disorders* **2010**, *3*, 379−389.

(15) Prayle, A.; Smyth, A. R. Aminoglycoside use in cystic fibrosis: therapeutic strategies and toxicity. *Curr. Opin. Pulm. Med.* **2010**, *16*, 604−610.

(16) Welch, E. M.; Barton, E. R.; Zhuo, J.; Tomizawa, Y.; Friesen, W. J.; Trifillis, P.; Paushkin, S.; Patel, M.; Trotta, C. R.; Hwang, S.; Wilde, R. G.; Karp, G.; Takasugi, J.; Chen, G.; Jones, S.; Ren, H.; Moon, Y. C.; Corson, D.; Turpoff, A. A.; Campbell, J. A.; Conn, M. M.; Khan, A.; Almstead, N. G.; Hedrick, J.; Mollin, A.; Risher, N.; Weetall, M.; Yeh, S.; Branstrom, A. A.; Colacino, J. M.; Babiak, J.; Ju, W. D.; Hirawat, S.; Northcutt, V. J.; Miller, L. L.; Spatrick, P.; He, F.; Kawana, M.; Feng, H.; Jacobson, A.; Peltz, S. W.; Sweeney, H. L. PTC124 targets genetic disorders caused by nonsense mutations. *Nature* **2007**, *447*, 87−91.

(17) Pace, A.; Pierro, P. The new era of 1,2,4-oxadiazoles. *Org. Biomol. Chem.* **2009**, *7*, 4337−4348.

(18) Boström, J.; Hogner, A.; Llinas, A.; Wellner, E.; Plowright, A. T. Oxadiazoles in Medicinal Chemistry. *J. Med. Chem.* **2012**, *55*, 1817−1830.

(19) Palumbo Piccionello, A.; Musumeci, R.; Cocuzza, C.; Fortuna, C. G.; Guarcello, A.; Pierro, P.; Pace, A. Synthesis and Preliminary Antibacterial Evaluation of Linezolid-like 1,2,4-Oxadiazole Derivatives. *Eur. J. Med. Chem.* **2012**, *50*, 441−448.

(20) Terenzi, A.; Barone, G.; Palumbo Piccionello, A.; Giorgi, G.; Guarcello, A.; Portanova, P.; Calvaruso, G.; Buscemi, S.; Vivona, N.; Pace, A. Synthesis, characterization, cellular uptake and interaction with native DNA of a bis(pyridyl)-1,2,4-oxadiazole copper(II) complex. *Dalton Trans.* **2010**, *39*, 9140−9145.

(21) Pibiri, I.; Pace, A.; Buscemi, S.; Causin, V.; Rastrelli, F.; Saielli, G. Oxadiazolyl-pyridines and perfluoroalkyl-carboxylic acids as building blocks for protic ionic liquids: crossing the thin line between ionic and hydrogen bonded materials. *Phys. Chem. Chem. Phys.* **2012**, *14*, 14306−14314.

(22) Lo Celso, F.; Pibiri, I.; Triolo, A.; Triolo, R.; Pace, A.; Buscemi, S.; Vivona, N. Study on the thermotropic properties of highly fluorinated 1,2,4-oxadiazolylpyridinium salts and their perspective applications as ionic liquid crystals. *J. Mater. Chem.* **2007**, *17*, 1201−1208.

(23) Palumbo Piccionello, A.; Guarcello, A.; Calabrese, A.; Pibiri, I.; Pace, A.; Buscemi, S. Synthesis of fluorinated oxadiazoles with gelation and oxygen storage ability. *Org. Biomol. Chem.* **2012**, *10*, 3044−3052.

(24) Pibiri, I.; Palumbo Piccionello, A.; Calabrese, A.; Buscemi, S.; Vivona, N.; Pace, A. Fluorescent Hg2+ Sensors: Synthesis and Evaluation of a Tren-Based Starburst Molecule Containing Fluorinated 1,2,4-Oxadiazoles. *Eur. J. Org. Chem.* **2010**, 4549−4553.

(25) Du, M.; Liu, X.; Welch, E. M.; Hirawat, S.; Peltz, S. W.; Bedwell, D. M. PTC124 is an orally bioavailable compound that promotes suppression of the human CFTR-G542X nonsense allele in a CF mouse model. *Proc. Natl. Acad. Sci. U.S.A.* **2008**, *105* (6), 2064−2069.

(26) Peltz, S. W.; Welch, E. M.; Jacobson, A.; Trotta, C. R.; Naryshkin, N.; Sweeney, H. L.; Bedwell, D. M. Nonsense suppression activity of PTC124 (ataluren). *Proc. Natl. Acad. Sci. U.S.A.* **2009**, *106*, E64.

(27) Kayali, R.; Ku, J.-M.; Khitrov, G.; Jung, M. E.; Prikhodko, O.; Bertoni, C. Readthrough compound 13 restores dystrophin expression and improves muscle function in the mdx mouse model for Duchenne muscular dystrophy. *Hum. Mol. Genet.* **2012**, *21*, 4007−4020.

(28) Peltz, S. W.; Welch, E. M.; Morsy, M.; Jacobson, A. Ataluren as an Agent for Therapeutic Nonsense Suppression. *Annu. Rev. Med.* **2013**, *64*, 407−425.

(29) Kerem, E.; Hirawat, S.; Armoni, S.; Yaakov, Y.; Shoseyov, D.; Cohen, M.; Nissim-Rafinia, M.; Blau, H.; Rivlin, J.; Aviram, M.; Elfring, G. L.; Northcutt, V. J.; Miller, L. L.; Kerem, B.; Wilschanski, M. Effectiveness of PTC124 treatment of cystic fibrosis caused by nonsense mutations: a prospective phase II trial. *Lancet* **2008**, *372*, 719−727.

(30) Hirawat, S.; Welch, E. M.; Elfring, G. L.; Northcutt, V. J.; Paushkin, S.; Hwang, S.; Leonard, E. M.; Almstead, N. G.; Ju, W.; Peltz, S. W.; Miller, L. L. Safety, tolerability, and pharmacokinetics of PTC124, a nonaminoglycoside nonsense mutation suppressor, following single- and multiple-dose administration to healthy male and female adult volunteers. *J. Clin. Pharmacol.* **2007**, *47*, 430−444.

(31) Mendell, J. R.; Rodino-Klapac, L.; Sahenk, Z.; Malik, V.; Kaspar, B. K.; Walker, C. M.; Clark, K. R. Gene therapy for muscular dystrophy: Lessons learned and path forward. *Neurosci. Lett.* **2012**, *527*, 90−99.

(32) Rowe, S. M.; Borowitz, D. S.; Burns, J. L.; Clancy, J. P.; Donaldson, S. H.; Retsch-Bogart, G.; Sagel, S. D.; Ramsey, B. W. Progress in cystic fibrosis and the CF Therapeutics Development Network. *Thorax* **2012**, *67*, 882−890.

(33) Kerem, E.; Wilschanski, M.; De Boeck, K.; Sermet-Gaudelus, I.; Constantine, S.; Elfring, G. L.; Miller, N. L.; Barth, J.; Ajayi, T. 65 Phase 3 study of ataluren (PTC124®) in nonsense mutation cystic fibrosis (nmCF): baseline data. *J. Cyst. Fibros.* **2011**, *10* (Suppl.1), S17.

(34) Rowe, S. M.; Miller, S.; Sorscher, E. J. Cystic fibrosis. *N. Engl. J. Med.* **2005**, *352*, 1992−2001.

(35) Kerem, E.; Kerem, B. Genotype-phenotype correlations in cystic fibrosis. *Pediatr. Pulmonol.* **1996**, *22*, 387−395.

(36) Lee, H.-L. R.; Dougherty, J. P. Pharmaceutical therapies to recode nonsense mutations in inherited diseases. *Pharm. Ther.* **2012**, *136*, 227−266.

(37) Auld, D. S.; Thorne, N.; Maguire, W. F.; Inglese, J. Mechanism of PTC124 activity in cell-based luciferase assays of nonsense codon suppression. *Proc. Natl. Acad. Sci. U.S.A.* **2009**, *106*, 3585−3590.

(38) Auld, D. S.; Lovell, S.; Thorne, N.; Lea, W. A.; Maloney, D. J.; Shen, M.; Rai, G.; Battaile, K. P.; Thomas, C. J.; Simeonov, A.; Hanzlik, P. R.; Inglese, J. Molecular basis for the high-affinity binding and stabilization of firefly luciferase by PTC124. *Proc. Natl. Acad. Sci. U.S.A.* **2010**, *107*, 4878−4883.

(39) Thorne, N.; Auld, D. S.; Inglese, J. Apparent activity in high-throughput screening: origins of compound-dependent assay interference. *Curr. Opin. Chem. Biol.* **2010**, *14*, 315−324.

(40) Thorne, N.; Inglese, J.; Auld, D. S. Illuminating Insights into Firefly Luciferase and Other Bioluminescent Reporters Used in Chemical Biology. *Chem. Biol.* **2010**, *17*, 646−657.

(41) Barbault, F.; Ren, B.; Rebehmed, J.; Teixeira, C.; Luo, Y.; Smila-Castro, O.; Maurel, F.; Fan, B. T.; Zhang, L.; Zhang, L. Flexible computational docking studies of new aminoglycosides targeting RNA 16S bacterial ribosome site. *Eur. J. Med. Chem.* **2008**, *43*, 1648−1656.

(42) Martinelli, J. R.; Watson, D. A.; Freckmann, D. M. M.; Barder, T. E.; Buchwald, S. L. Palladium-Catalyzed Carbonylation Reactions of Aryl Bromides at Atmospheric Pressure: A General System Based on Xantphos. *J. Org. Chem.* **2008**, *73*, 7102−7107.

(43) Kanda, T.; Sullivan, K. F.; Wahl, G. M. Histone-GFP fusion protein enables sensitive analysis of chromosome dynamics in living mammalian cells. *Curr. Biol.* **1998**, *8*, 377−385.

(44) Thorpe, P. H.; Stevenson, B. J.; Porteous, D. J. Functional correction of episomal mutations with short DNA fragments and RNA-DNA oligonucleotides. *J. Gene Med.* **2002**, *4*, 195−204.

(45) Kwok, S.; Kellogg, D. E.; Mckinney, N.; Spasic, D.; Goda, L.; Levenson, C.; Sninsky, J. J. Effects of Primer Template Mismatches on the Polymerase Chain-Reaction-Human-Immunodeficiency-Virus Type-1 Model Studies. *Nucleic Acids Res.* **1990**, *18*, 999−1005.

(46) Lentini, L.; Barra, V.; Schillaci, T.; Di Leonardo, A. MAD2 depletion triggers premature cellular senescence in human primary fibroblasts by activating a p53 pathway preventing aneuploid cells propagation. *J. Cell. Physiol.* **2012**, *227* (9), 3324−3332.

(47) Ponder, J. W. *TINKER 4.2*, Software Tools for Molecular Design; http://dasher.wustl.edu/tinker.

(48) Ruiz, R.; Garcia, B.; Ruisi, G.; Silvestri, A.; Barone, G. Computational study of the interaction of proflavine with d-(ATATATATAT)(2) and d(GCGCGCGCGC)(2). *J. Mol. Struct.: THEOCHEM* **2009**, *915*, 86−92.

(49) Spinello, A.; Terenzi, A.; Barone, G. Metal Complex-DNA Binding: Insights from Molecular Dynamics and DFT/MM Calculations. *J. Inorg. Biochem.* **2013**, *124*, 63−69.

(50) Sousa Da Silva, A. W.; Vranken, W. F.; Laue, E. D. ACPYPE - Antechamber python parser interface. *BMC Res. Notes* **2012**, *5*, 367.

(51) Wang, J. M.; Wang, W.; Kollman, P. A.; Case, D. A. Automatic atom type and bond type perception in molecular mechanical calculations. *J. Mol. Graph. Model.* **2006**, *25*, 247−260.

(52) Wang, J. M.; Wolf, R. M.; Caldwell, J. W.; Kollman, P. A.; Case, D. A. Development and testing of a general amber force field. *J. Comput. Chem.* **2004**, *25*, 1157−1174.
(53) Hess, B.; Kutzner, C.; van der Spoel, D.; Lindahl, E. GROMACS 4: Algorithms for highly efficient, load-balanced, and scalable molecular simulation. *J. Chem. Theory Comput.* **2008**, *4*, 435−447.
(54) Van der Spoel, D.; Lindahl, E.; Hess, B.; Groenhof, G.; Mark, A. E.; Berendsen, H. J. C. GROMACS: Fast, flexible, and free. *J. Comput. Chem.* **2005**, *26*, 1701−1718.
(55) Perez, A.; Marchan, I.; Svozil, D.; Sponer, J.; Cheatham, T. E.; Laughton, C. A.; Orozco, M. Refinement of the AMBER force field for nucleic acids: improving the description of alpha/gamma conformers. *Biophys. J.* **2007**, *92*, 3817−3829.
(56) Guy, A. T.; Piggot, T. J.; Khalid, S. Single-stranded DNA within nanopores: conformational dynamics and implications for sequencing; a molecular dynamics simulation study. *Biophys. J.* **2012**, *103*, 1028−1036.
(57) *Maestro*, version 9.3; Schrödinger, LLC: New York, NY, 2012.
(58) Bussi, G.; Donadio, D.; Parrinello, M. Canonical sampling through velocity rescaling. *J. Chem. Phys.* **2007**, *126*, 014101.
(59) Darden, T.; York, D.; Pedersen, L. Particle mesh Ewald: An N·log(N) method for Ewald sums in large systems. *J. Chem. Phys.* **1993**, *98*, 10089.
(60) Pace, A.; Buscemi, S.; Vivona, N. The synthesis of fluorinated heteroaromatic compounds. Part 1. Five-membered rings with more than two heteroatoms. A review. *Org. Prep. Proc. Int.* **2005**, *37*, 447−506.
(61) Terenzi, A.; Barone, G.; Palumbo Piccionello, A.; Giorgi, G.; Guarcello, A.; Pace, A. Synthesis and chemical characterization of $Cu^{II}$, $Ni^{II}$ and $Zn^{II}$ complexes of 3,5-bis(2′-pyridyl)-1,2,4-oxadiazole and 3-(2′-pyridyl)5-(phenyl)-1,2,4-oxadiazole ligands. *Inorg. Chim. Acta* **2011**, *373*, 62−67.
(62) Buscemi, S.; Pace, A.; Palumbo Piccionello, A.; Vivona, N. Synthesis of fluorinated first generation starburst molecules containing a triethanolamine core and 1,2,4-oxadiazoles. *J. Fluor. Chem.* **2006**, *127*, 1601−1605.
(63) Palumbo Piccionello, A.; Pace, A.; Buscemi, S.; Vivona, N. 1,2,4-Oxadiazole Rearrangements Involving an NNC Side-Chain Sequence. *Org. Lett.* **2009**, *11*, 4018−4020.
(64) Palumbo Piccionello, A.; Buscemi, S.; Vivona, N.; Pace, A. Exploiting the CNC Side Chain in Heterocyclic Rearrangements: Synthesis of 4(5)-Acylamino-imidazoles. *Org. Lett.* **2010**, *12*, 3491−3493.
(65) Buscemi, S.; Pace, A.; Palumbo Piccionello, A.; Pibiri, I.; Vivona, N. Fluorinated heterocyclic compounds. A photochemical approach to a synthesis of fluorinated quinazolin-4-ones. *Heterocycles* **2004**, *63*, 1619−1628.
(66) Palumbo Piccionello, A.; Pace, A.; Pibiri, I.; Buscemi, S.; Vivona, N. Synthesis of fluorinated indazoles through ANRORC-like rearrangement of 1,2,4-oxadiazoles with hydrazine. *Tetrahedron* **2006**, *62*, 8792−8797.
(67) Pace, A.; Pibiri, I.; Buscemi, S.; Vivona, N. Photochemistry of Fluorinated Heterocyclic Compounds. An Expedient Route for the Synthesis of Fluorinated 1,3,4-Oxadiazoles and 1,2,4-Triazoles. *J. Org. Chem.* **2004**, *69*, 4108−4115.
(68) Buscemi, S.; Vivona, N.; Caronna, T. A generalized and effcicient synthesis of 3-amino-, 3-(*N*-alkylamino)-, 3-(*N*,*N*-dialkylamino)-5-alkyl-1,2,4-oxadiazoles by irradiation of 3-alkanoylamino-4-phenyl-1,2,5-oxadiazoles (furazans). *Synthesis* **1995**, 917−919.
(69) Amato, A.; Schillaci, T.; Lentini, L.; Di Leonardo, A. CENPA overexpression promotes genome instability in pRb-depleted human cells. *Mol. Cancer* **2009**, *8*, 119.
(70) Heier, C. R.; DiDonato, C. J. Translational readthrough by the aminoglycoside Geneticin (G418) modulates SMN stability in vitro and improves motor function in SMA mice in vivo. *Hum. Mol. Genet.* **2009**, *18*, 1310−1322.
(71) Youngman, E. M.; McDonald, M. E.; Green, R. Peptide release on the ribosome: mechanism and implications for translational control. *Annu. Rev. Microbiol.* **2008**, *62*, 353−373.
(72) This article was published after the first submission date of the present manuscript: McElroy, S. P.; Nomura, T.; Torrie, L. S.; Warbrick, E.; Gartner, U.; Wood, G.; McLean, W. H. I. A lack of premature termination codon read-through efficacy of PTC124 (Ataluren) in a diverse array of reporter assays. *PLoS Biol.* **2013**, *11*, e1001593.